

WET-SNOW AVALANCHE INTERACTING WITH A DEFLECTING DAM: FIELD OBSERVATIONS

Betty Sovilla<sup>1</sup>, Ilaria Sonatore<sup>1,2</sup>, Stefan Margreth<sup>1</sup> and Marc Christen<sup>1</sup>

<sup>1</sup>WSL Institute for Snow and Avalanche Research SLF, Flüelastrasse 11, Davos Dorf, 7260, Switzerland

<sup>2</sup>Università degli Studi di Milano - Bicocca, Dipartimento di Scienze Geologiche e Geotecnologie, Piazza della Scienza 4, Milano 20126, Italy

**ABSTRACT:** In 2008 a large wet-snow avalanche occurred in the region of Klosters, Switzerland. The avalanche reached the valley bottom and interacted with a deflecting dam that was constructed after the avalanche winter 1999, overflowing it at its lower end. To document this extraordinary event, we performed airborne laser-scanning immediately after the avalanche. This data, together with a video sequence made during the avalanche descent, provided a unique data set to study the dynamics of a wet-snow avalanche and its flow behavior around the deflecting dam. The avalanche hit the dam with deflecting angles of 10-30°. We could observe that, for smaller deflecting angles, the friction of the avalanche as it flowed alongside the dam slowed down the avalanche front, but, for higher deflecting angles, the avalanche suddenly accelerated increasing its run-out distance. Additionally, we could observe that snow deposits left by the avalanche exhibited strong pattern formation, which reflected the history of the wet flow. In particular, we could detect high levees running parallel to the curvature of the dam indicating the dam influenced the lateral spreading and we estimated that the whole deposit area was deviated from its original direction by approximately 25°. Furthermore, we observed the formation of numerous rolls-waves, which increased the avalanche flow depth and caused the overflow of the dam. Based on our analysis, we propose recommendations to take into account the effects of wet-snow avalanche flow for practical design of deflecting dams.

**KEYWORDS:** Wet-snow avalanche, Avalanche deflecting dam, Airborne laser-scanning,

## 1. INTRODUCTION

On the 23<sup>rd</sup> of April 2008, a large wet-snow avalanche naturally released at Gatschiefer, Canton Grisons, Switzerland. The avalanche

-----  
\* *Corresponding author address:* Betty Sovilla, WSL, Swiss Federal Institute for Snow and Avalanche Research Flüelastrasse, 11, CH-7260 Davos Dorf; tel: +41-81-417 02 63; fax: +41-81-417 01 10; email: [sovilla@slf.ch](mailto:sovilla@slf.ch).

reached the valley bottom with an unexpected long run-out and interacted with a deflecting dam that was constructed after the avalanche winter of 1999, overflowing it at its downward end (Figure 1).

Deflecting dams are often designed to deviate dry snow avalanches, which are considered to be determining for the design because of the high velocities (Jóhannesson et al., 2009; Baillifard, 2007). If necessary, flow depths and deposit

heights of wet-snow avalanches are considered in the design as well, typically by expert judgement, because the current avalanche dynamics models often fail in such situations.

Recent investigations verify that wet-snow avalanches have enormous destructive forces in spite of small velocities (Sovilla et al., 2010; Sovilla et al., 2008; Baroudi et al., submitted). Furthermore, compared to dense flow avalanches, they have larger flow depths and tend to spread more laterally following small terrain irregularities regardless of their original direction, and thus may become decisive for hazard mapping and realisation of mitigation measures.

Studies concerning wet-snow avalanches are relatively limited as well as those regarding the interaction between avalanches with dams (Jóhannesson, 2001). For a better understanding of the wet-snow avalanche dynamics and the interaction with protection structures, the Gatschiefer avalanche was investigated in detail. Luckily, the event was also filmed from the opposite side of the valley. The excellent dataset on the Gatschiefer avalanche event was the starting point of our analysis.

## 2. DATA ACQUISITION METHODS

### 2.1 Airborne laser-scanning

An airborne laser-scanning survey was performed three days after the avalanche release. The survey allowed the automatic extraction of a high resolution digital snow surface model, providing a way to measure the surface of snow accurately without any ground control point and independently of the contrast of the snow. Measurements extended over the entire avalanche path with a spatial resolution of 0.5 m and a total vertical accuracy of 0.1 m. For more detailed information on airborne laser-scanning for snow depth measurements see Sovilla et al. (2010).

In order to measure the snow depth variability in the avalanche path, the snow surface of the area is mapped generally before (coordinate  $z_1$ ) and after the triggering (coordinate  $z_2$ ). Thus, net erosion and deposition can be calculated by subtracting these two depths directly (Sovilla et al., 2010):

$$h_s = z_1 - z_2$$

In our case the avalanche released spontaneously making it impossible to measure the snow surface

before the event. The calculation of the snow depth,  $h_s$ , was approximated by directly subtracting from the  $z_2$  coordinates the summer digital terrain model coordinates,  $z_s$ . This approximation did not affect substantially the final results because the avalanche sliding surface was directly on the ground (Figure 2 and Figure 4). The summer digital terrain model had a resolution of 2.5 m and accuracy of 0.5 m in open terrain. Thus, we estimate the final accuracy of the snow depth,  $h_s$ , to be in the order of  $\pm 0.5$  m.

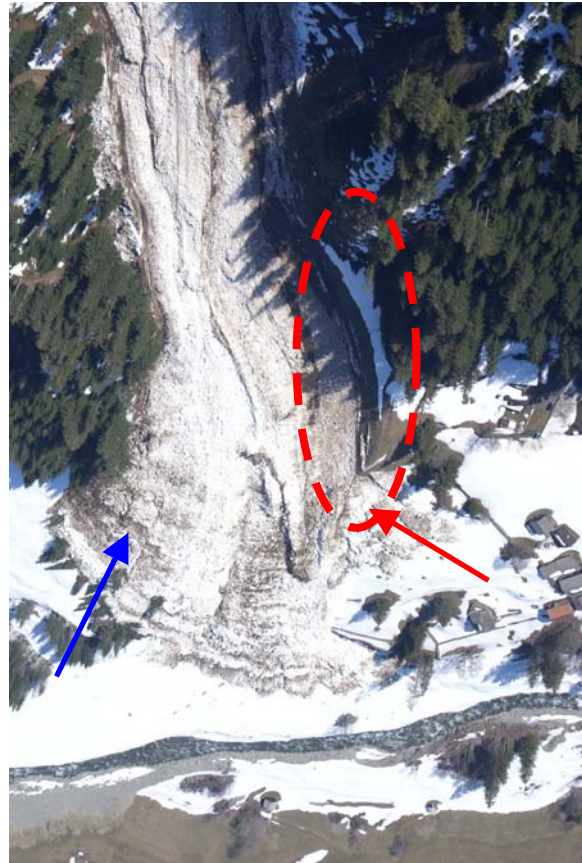


Figure 1. Lower deposition zone of the Gatschiefer avalanche. The red circle indicates the dam location. The blue arrow indicates the lateral spreading of the avalanche where several trees were uprooted. The red arrow indicates the point where the avalanche overflowed the dam.

### 2.2 Video analysis

The Gatschiefer avalanche was occasionally filmed from the opposite side of the valley by a passing bus driver using a cell phone (the video can be seen on YouTube <http://www.youtube.com/watch?v=kgY43LZ8o94>). The video shows the run-out zone of the

avalanche from an altitude of 1500 m a.s.l. where two flow channels converge, to an altitude of 1100m a.s.l. corresponding to the valley bottom, near the river Landquart (Figure 1).

The video has been scanned every 10 seconds, and analyzed focusing on fronts and roll-waves propagation. Video frames have been used to investigate the avalanche flow direction, its velocity, and the interaction with the deflecting dam.



Figure 2. Release zone #1. The Gatschiefer avalanche released directly on the ground.

### 3. THE GATSCHIEFER AVALANCHE DEFLECTING DAM

During the catastrophic winter 1999, a large avalanche reached several houses located in the run-out zone of the Gaschiefer avalanche path (Figure 3). A 5-7 m high and 140 m long deflecting dam was constructed in 2003 to deflect avalanches away from the settlement. The positioning of the dam was difficult because the deflected avalanche should not increase the hazard of the houses in the "Brosi" area.

The height of the deflecting dam was calculated using the traditional equation:

$$H_D = h_u + h_f + h_s, \quad [1]$$

where  $h_u$  is the run-up height,  $h_f$  is the thickness of the flowing dense core and  $h_s$  is the thickness of the snow cover and previous avalanche deposits in front of the dam. The term  $h_u$  was computed according to the equation:

$$h_u = \frac{(u \sin \varphi)^2}{2g\lambda}, \quad [2]$$

where  $u$  is the velocity of the design avalanche at the dam location,  $\varphi$  is the deflecting angle of the dam,  $g$  is the gravity acceleration and  $\lambda$  is an empirical parameter that describe the energy loss during the impact with the dam (Salm et al., 1990; Lied and Kristensen. 2003, Norem, 2004). A dry-dense flow was chosen as a design avalanche. The  $\lambda$  parameter was chosen to be 1.

By comparing the outlines of the 1999 and 2008 avalanches we could estimate the effective dam deflecting angles,  $\varphi$ , to vary between 10° and 30° (Figure 3).

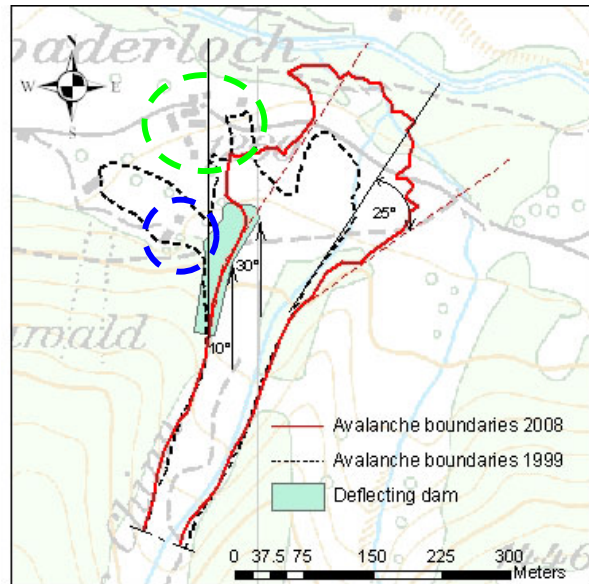


Figure 3. Outlines of the 1999 avalanche (black dashed line) and of the 2008 avalanche (red line). The buildings in the blue circle were heavily damaged in 1999. The buildings in the green circle ("Brosi" area) were not damaged. Arrows indicate the main flow direction of the 1999 avalanche; the left red dotted line shows the local direction of the dam axis. Note that, it also coincides with the 2008 avalanche main flow direction. The right red dotted line shows the maximum lateral spreading of the 2008 avalanche.

Figure 3 shows that the dam was able to deviate the 2008 avalanche away from the buildings damaged in 1999. Without the dam the avalanche would probably have reached again the settlement. However, we think that the dam height, designed to deviate a dry-dense avalanche, was underestimated for the deviation of an extreme wet-snow avalanche. The snow traces left by the avalanche on the dam showed that the avalanche flow equaled the dam height (Figure 4). Nevertheless, the avalanche overrun only the

lower end of the dam which is slightly smaller and stopped close by the houses in the “Brosi” area (Figure 1).



Figure 4. Avalanche run-up along the dam side facing the avalanche. Beside the dam location, the ground was the sliding surface of the avalanche.

#### 4. DATA ANALYSIS

##### 4.1 The Gatschiefer avalanche and its mass balance

Two release areas have been identified from laser-scanning measurements. Both areas were characterized by well defined fracture and stauwall lines.

Release zone #1 was situated in a non-vegetated, area between 2'100 and 2'300 m a.s.l.. The area was 140'000 m<sup>2</sup>, the length was ≈600 m and the mean inclination was 38°.

The much smaller release zone #2 was located between 1'900 and 2'000 m a.s.l.. The area was 21'000 m<sup>2</sup> and the fracture line extended over a length of ≈200 m. Its mean inclination was 43°.

Both release areas moved as a slab, which involved the whole snow cover (Figure 2 and Figure 5). Information on snow cover depth before the avalanche release have been deduced from laser-scanning measurements in areas adjacent to the starting zones, where the snow was not influenced by avalanches. Snow cover depths near the upper and lower starting zones were ≈2.2 m and ≈2 m, corresponding to volumes of 308'000 m<sup>3</sup> and 42'000 m<sup>3</sup> for release #1 and #2, respectively.

Immediately below release #1, a small terrace enhanced the deposition of around 224'000 m<sup>3</sup> of snow. This volume corresponds to ≈70% of release #1. Thus only approximately 126'000 m<sup>3</sup> of snow from both release areas were canalized in

the flowing zone. The avalanche flow split in two vegetated gullies characterised by a mean slope of 30°. The two gullies converge at an elevation 1500 m a.s.l. at which point the combined flow entered a wide (W=100m) 400 m long, non-vegetated run-out segment characterized by a mean slope of some 15° (Figure 5). Two meandering flow channels are observed at the beginning of this segment; however, the video reveal that the flow combined and then flowed with a surprisingly regular and strait flow front extending over the entire 100 m channel width.

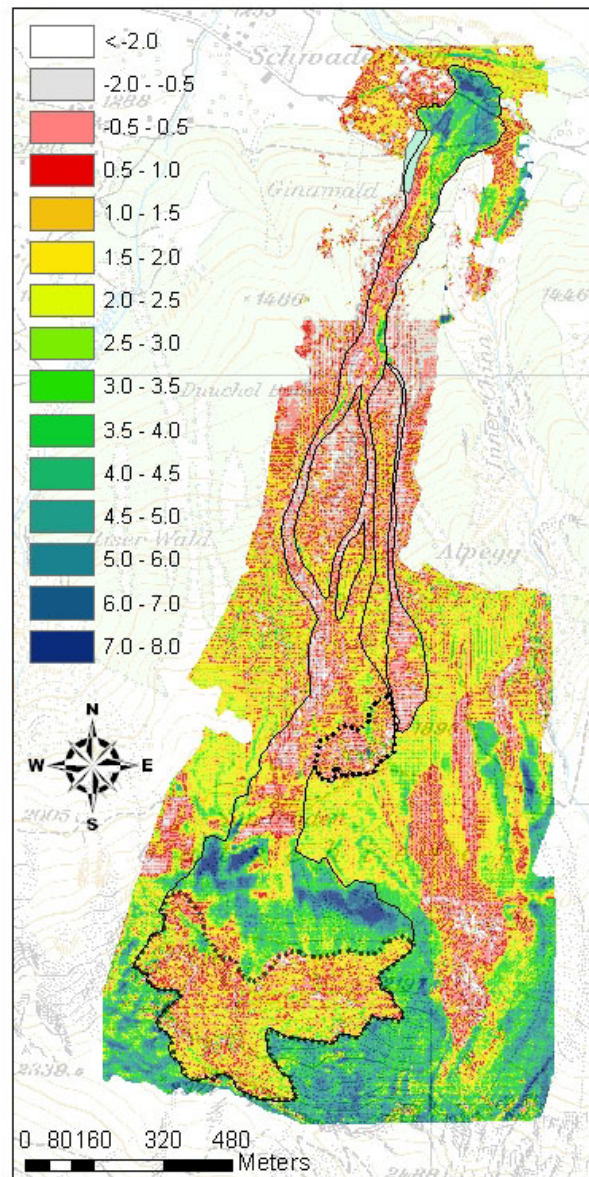


Figure 5. Calculated snow depths in the Gatschiefer avalanche track after the event of April 2008. Dotted contours shows release zones #1 (larger area) and #2 (smaller area).

Table 1. Mass balance of the Gatschiefer avalanche of 23 April 2008.

Avalanche release	Release area (m <sup>2</sup> )	Estimated Fracture depth (m)	Release volume (m <sup>3</sup> )	Estimated release density (Kg/m <sup>3</sup> )	Release Mass (t)
No.1	140'000	2.2	308'000	300	≈92'000
No.2	21'000	2.0	42'000	300	≈13'000
Avalanche deposition	Deposition area (m <sup>2</sup> )	Mean/max deposition depth (m)	Deposition volume (m <sup>3</sup> )	Estimated deposition density (Kg/m <sup>3</sup> )	Deposition mass (t)
Upper	56'000	4,0/13	224'000	300	≈67'000
Lower	53'000	2.6/11.8	137'800	500	≈69'000

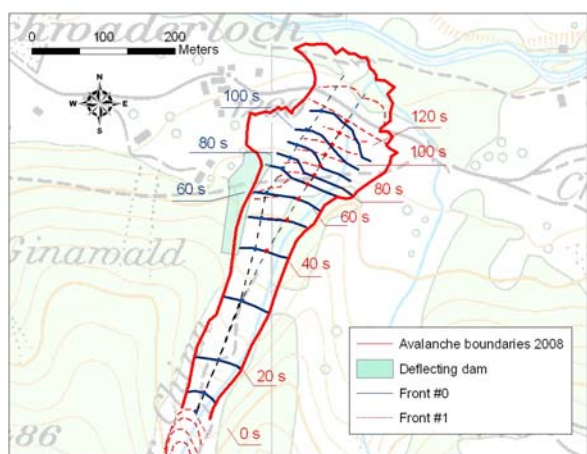


Figure 6. Gatschiefer avalanche of 23 April 2008. Avalanche front locations at 10 s intervals from video sequences. Blue lines show the position of the most advanced avalanche front (front #0) while red dashed lines show the position of front #1.

At the end of this track segment, on the left flow side of the channel, the avalanche struck the deflecting dam (Figure 1 and Figure 5), overflowing it slightly at its downward end. The avalanche entered a forest stand opposite the dam and several spruce trees (diameter  $d=0.60\text{m}$ ; age greater than 100 years) were fractured, overturned or uprooted by the slow moving mass (Figure 1).

The avalanche did not reach the river Landquart, but it did descend the steep banks. From laser-scanning measurements, the estimated area of the lower deposition zone was  $53'000\text{ m}^2$  with mean and maximum deposition depths of 2.6 and 11.8 m, respectively. The final deposition volume has been estimated to be  $137'800\text{ m}^3$ , very similar to the initial avalanche volume. The avalanche

eroded the whole snowpack along the avalanche path, but the limited potential erosion area (the avalanche remained confined in very narrow channels) has controlled the volume increase during the flow. However, due to the densification of the snow along the avalanche path (estimated density increase from  $300$  to  $500\text{ kg/m}^3$ ) the avalanche mass was approximately double (Sovilla et al., 2006).

#### 4.2 Avalanche fronts and roll-waves velocities

Avalanche velocities have been deduced from video sequences taken every 10 seconds, focusing on the wave fronts propagation in the run-out and deposition zones. The wave fronts were easily recognizable because of their higher and dirtier wave head.

The first wave front entering the run-out zone has been appointed as front #1 (Figure 6). We could observe numerous roll-waves following front #1. Part of these roll-waves disappeared before reaching the main front, while some others flowed slightly faster than the front #1, reaching and merging with it before the dam was hit. Their generation seemed to correspond to the impact with small surface bumps.

The impact with the deflecting dam originated a sort of large snow cloud and the formation of two additional waves that overtook front #1 and spread laterally to the right in direction of the forest. These new fronts were appointed as front #2 and front #3, respectively.

The most advanced avalanche front (front #0) is the result of the merging of fronts #1, #2 and #3 and it is indicated in Figure 6 in blue.

Velocity has been calculated along two longitudinal profiles (Figure 6). The red profile follows front #1 and it represents the flow velocity

far from the deflecting dam. The blue profile follows front #0, it is traced close to the deflecting dam, and should represent the influence of the dam on the avalanche dynamics.

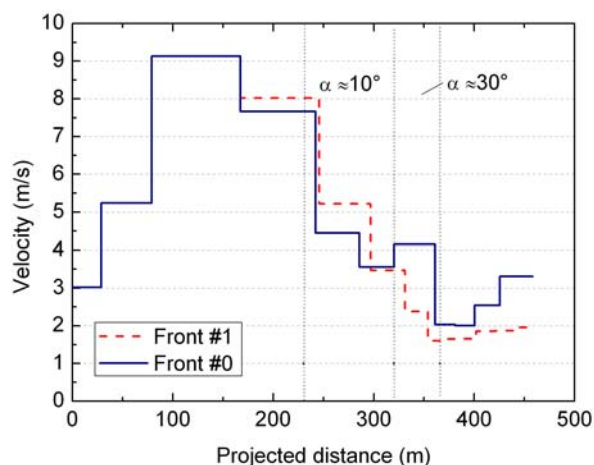


Figure 7. Avalanche front velocity according to the longitudinal profiles shown in Figure 6. The red line shows the average velocity of front #1, while the blue line shows the average velocity of front #0.

The red dashed line in Figure 7 shows the front #1 velocity. From 1370 m a.s.l. (indicated as 0 s in Figure 6) velocity progressively increased to reach a maximum of  $\approx 9 \text{ ms}^{-1}$ . After being reached by the roll-wave fronts the velocity decreases to a minimum of about  $2 \text{ ms}^{-1}$ . Afterwards the avalanche kept constant velocity and crossed the road near the Landquart river, jumping down to the river bed and stopping.

The fronts travelling close to the dam (blue profile) showed a different behaviour. The avalanche reached the deflecting dam with a velocity of  $\approx 8 \text{ ms}^{-1}$  (Figure 7). We estimated that, initially, the avalanche was deflected by the dam with  $\approx 10^\circ$ . At this stage, the friction of the avalanche as it flowed along the dam slowed down front #1 in respect to the corresponding point on the red profile (Figure 7). Then the avalanche entered the lower section of the dam which deviated the flow by  $\approx 30^\circ$ . Here we could observe a deceleration of front #1 and, simultaneously, the formation of two new fronts. The new fronts accelerated up to  $4 \text{ ms}^{-1}$ , and overtook front 1# over the all avalanche width.

#### 4.3 Avalanche flow depth, run-up depth and snowcover-deposit depth

The maximum height reached by the avalanche along the dam could be deduced from the traces left by the flow on the dam embankment (Figure 4). Traces indicated flow heights to be higher than 5 m.

As eq. 1 suggests, the maximum flow depth may be given by the sum of different factors including the snow cover depth and former avalanche deposits,  $h_s$ , the run-up height,  $h_u$ , and the avalanche core depth  $h_f$ .

Figure 4 shows that the avalanche glided directly on the ground and it eroded all snow cover in front of the dam. Additionally, we did not observe previous avalanche deposits. Thus, in this case the term  $h_s$  was negligible.

The avalanche reached the dam with a velocity of about  $8 \text{ ms}^{-1}$ . Assuming a minimum flow depth of 5 m, and a dam deviation angle of  $10^\circ$ , using eq. 2 we could estimate a run-up height of about 0.5m, and thus, also run-up height  $h_u$  were not relevant in this case. Additionally, the Froude number just before impact was around 1, i.e. the avalanche was close to a sub-critical flow and thus there was not the condition for the formation of a shock wave which would have substantially increased the avalanche depth (Jóhannesson et al., 2009).

Thus, the thickness of the wet-snow avalanche dense core, which was increased by the presence of numerous surface roll-waves, was decisive for the interaction with the deflecting dam.

#### 4.4 Flow direction and lateral spreading

Laser-scanning measurements (Figure 8) and aerial photographs (Figure 1) showed a common channelled pattern in the run-out and lower deposition zones with levees morphology.

These shapes are easily recognizable from their characteristic pattern: lateral static edges corresponding to the borders of the flow, and a central zone, generally lower in depth, corresponding to the flow drainage. Levees were made of large snow clods covered with dirt on each border of the flow, and at few location, in the drainage channel, the ground was exposed (Figure 4), indicating that the avalanche glided directly on the ground.

Near the dam, all levees were diverted to the right (Figure 8) following a direction almost parallel to the dam curvature and suggesting the deflecting dam had a strong influence on the lateral avalanche spreading.

From the summer DTM, we could determine the steepest descent at each location in the deposition zone (blue lines in Figure 9). While the 1999

avalanche followed the steepest descent, the 2008 avalanche followed a direction with diverted flow lines up to  $45^\circ$  in respect to the steepest descent. The whole deposit area was deviated toward the forest by ca.  $25^\circ$  (Figure 3).

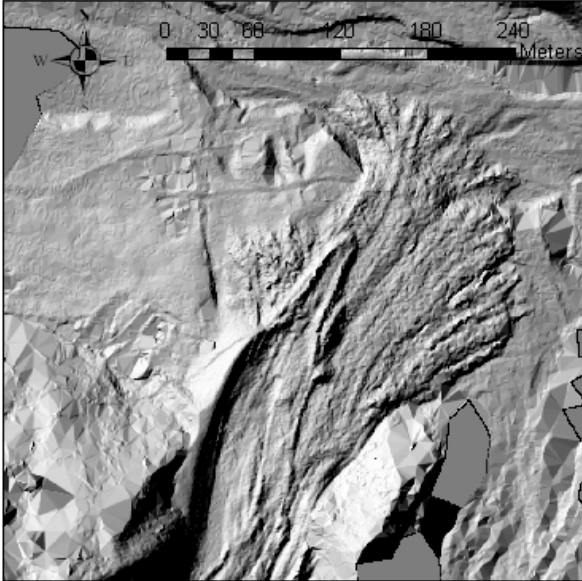


Figure 8. Hillshade of the lower deposition zone of the Gatschiefer avalanche of 23 April 2008 from laser-scanning measurements. The flow direction is highlighted by the presence of numerous leaves.

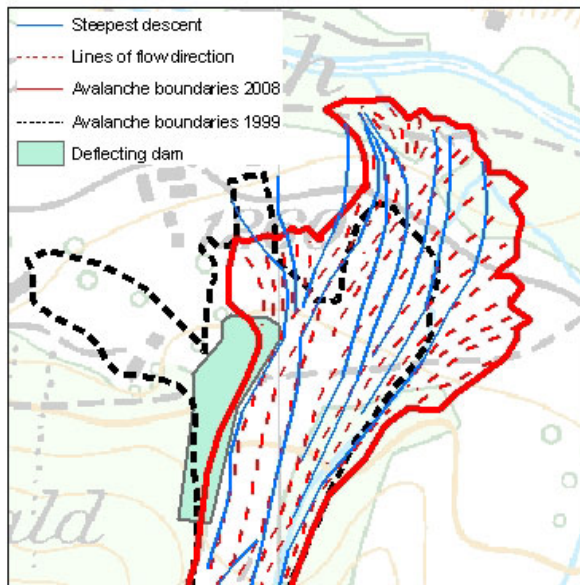


Figure 9. Comparison between flow lines of the 2008 avalanche (dashed red lines) and the direction of the steepest descent (blue lines).

## 5. CONCLUSIONS

Laser-scanning measurements and video analysis showed interesting details of the wet-snow avalanche flow and its interaction with the deflecting dam. Our preliminary results may be summarized as follow:

- This extreme wet-snow avalanche was characterized by large flow depths, further increased by the presence of numerous roll-waves. Because of the very small avalanche velocity, the run-up height on the dam was negligible. Thus, for the design of deflecting dam taking into account wet-snow avalanche flow it is crucial to predict correct flow depths. Further, the development process of roll-waves should be understood in order to predict their occurrence, depth and velocity. In case of multiple avalanche events (which will reduce the effective height of the dam) or for larger avalanche volumes the dam height, designed for a dry-dense avalanche, may not be sufficient.
- The deflecting dam deviated the avalanche flow from  $10^\circ$  to  $30^\circ$ . For the smaller deflecting angle ( $10^\circ$ ) we could observe a deceleration of the flow probably given by the friction between the avalanche and the dam embankment, but as soon as the avalanche reached the larger deflecting angle ( $30^\circ$ ) we could observe a more complex interaction which, finally produced an acceleration of the flow by about 50% and thus, an increase in the run-out distance. We do not know the exact reasons for the deceleration and acceleration of the avalanche flow along the deflecting dam. For a better understanding of the flow behavior of wet-snow avalanches in the runout zone further investigations are required.
- The curvature of the flow lines in the deposition zone run parallel to the curvature of the dam suggesting that the dam was able to influence the avalanche flow over the entire avalanche width. We could observe that the dam shifted the whole avalanche body by about  $25^\circ$  toward the forest, by changing the flow direction up to  $45^\circ$  in respect to the topography steepest descent. This behavior may be typical for wet-snow avalanche flow, and not for dry-dense flow. Nevertheless, it is important to improve our knowledge about lateral spreading and introduce it into three-

dimensional numerical models to be able to correctly predict the influence of dams in avalanche hazard mapping.

These preliminary results give an overview of important processes which need to be better investigated to improve the design approach for deflecting dams.

Airborne laser-scanning proved to be an effective technique to gather detailed information concerning the extent, run-out distances, deposition heights and general flow behavior of an avalanche. The accuracy of the measurements in the deposition zone (about 0.1 m) allowed to study the interaction of the avalanche with the dam in detail. Thus, in future we recommend to use this technique to collect additional data.

## 7. ACKNOWLEDGEMENTS

Part of the funding for this research has been provided by the Swiss Federal Office for the Environment (FOEN) and by the Office for Forest, section Natural Hazards, of Canton Grisons. The authors would like to thank the avalanche dynamics team for their support in the field campaign.

## 8. REFERENCES

Baillifard, M.-A., 2007. Interaction between snow avalanches and catching dams, Ph.D.thesis, ETHZ, Zürich.

Baroudi, D., B. Sovilla and E. Thibert, submitted. Effects of flow regime and sensor geometry on snow avalanche impact pressure measurements. Submitted to J. Glaciol.

Jóhannesson, T., P. Gauer, D. Issler and K. Lied. 2009. The design of avalanche protection dams. Report of the European commission.

Jóhannesson, T., 2001. Run-up of two avalanches on the deflecting dams at Flateyri, north-western Iceland, *Ann. Glaciol.*, 32: 350-354.

Lied, K., and K. Kristensen. 2003. *Snøskred. Håndbok om Snøskred*, Vett & Viten as., Oslo.

Norem, H. 1994. *Snow Engineering for Roads*, *Tech. rep.*, Norwegian Public Roads Administration, Oslo.

Salm, B., Burkard, A. and Gubler, H., 1990.

Berechnung von Fließlawinen: eine Anleitung für Praktiker mit Beispielen. Eidg. Inst. Schnee und Lawinenvorsch. Mitt. 47.

Sovilla B, Burlando P, Bartelt P., 2006. Field experiments and numerical modeling of mass entrainment in snow avalanches. *J. Geophys. Res.*, 11, F03007.

Sovilla, B, M. Schaer, M. Kern M and P. Bartelt, 2008. Impact pressures and flow regimes in dense snow avalanches observed at the Vallée de la Sionne test site. *J. Geophys. Res.*, 113: F01010.

Sovilla, B., M. Kern and M. Schaer, 2010. Slow drag in wet avalanche flow, *Journal of Glaciology*, 56(198): 587-592.

Sovilla, B., J. N. McElwaine, M. Schaer, and J. Vallet, 2010. Variation of deposition depth with slope angle in snow avalanches: Measurements from Vallée de la Sionne. *J. Geophys. Res.*, 115: F02016, doi:10.1029/2009JF001390.